Potential Distribution in a Two-emitter Diode

MANFRED TROPPMANN

Institut für Plasmaphysik GmbH, Garching near Munich, Federal Republic of Germany

(Z. Naturforsch. **25 a**, 504—518 [1970]; received 21 January 1970)

The existing model of a "collisionless" alkali plasma diode is extended including the case of two incandescent plane electrodes emitting electrons as well as ions with a half-Maxwellian velocity distribution. The potential distributions within the diode space derived from this theory are examined in detail. Physically necessary conditions reduce the well-known ambiguity of solutions to a single one (with uniform plasma potential) at a given set of parameters. Further solutions, corresponding to spatially oscillatory potential shapes which are consistent with the collisionless theory, disappear if the ion-ion collision probability within the diode plasma exceeds 0.1 per emitter distance.

In the experiment the potential distributions are scanned using a new electron beam probing technique. The results agree with the theory.

1. Introduction

In the past the discussion of the potential distribution in a plasma diode with two emitters yielded contradictionary results. A number of authors, e. g. [1] reported the potential curve to be monotonic within each of the emitter sheaths in the case of ion rich emission, whereas in another paper [2] a double sheath in front of the negative emitter was found. Other aspects concerning the ambiguity of the solutions of the present problem and the existence of spatially oscillatory potential distributions [1, 2] were not yet clear.

The reason for these contradictions had not been clarified up to now. Therefore, the present work starts from the basis of all discussions concerning potential shapes, the Poisson-equation, and gives a detailed investigation of its solutions. In doing so the boundary conditions are appropriated to a two-emitter diode. The problem, however, is not accessible to theoretical treatment without a number of assumptions [3, 4] which are relatively well covered by the experimental conditions.

The one-dimensional model consists of two planar electrodes facing each other (Fig. 1). The diameter of the plates is much larger than their distance. They are heated to equal temperatures ($T_p = T_I = T_{II}$). Electrons and ions leave the electrodes with half-Maxwellian velocity distributions corresponding to a temperature equal to the plate temperature [5] ($T_- = T_+ = T_p$). The work function of the electrodes is asumed to be equal and uniform over the surface. The mean free paths for encounters between plasma particles are large compared with the Debye-length and with the diode spacing.

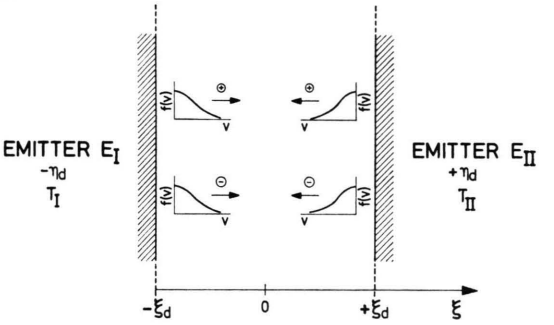

Fig. 1. The model used for calculations.

In the first part of the paper, trapping of charge carriers near the potential extrema is left out of consideration, i. e. the diode is assumed to be *ideally* collisionless. In a second part, the effect of particle trapping, arising from a finite collision probability, will be discussed qualitatively.

Poisson's equation in a form appropriate to the model of the plasma diode reads

$$d^2V/dx^2 = 4\pi e\{\vec{N}_-(x) + \overleftarrow{N}_-(x) - \vec{N}_+(x) - \overleftarrow{N}_+(x)\}, \quad (1)$$

where the local particle density $N(x)$ is separated into the contributions from particles flowing in the $+x$ and $-x$ directions, respectively.

Sonderdruckanforderungen an Frau Dr. L. JOHANNSEN, Institut für Plasmaphysik GmbH, Bibliothek, *D-8046 Garching* bei München.

[1] A. SESTERO and M. ZANNETTI, Nuovo Cim. **51**, 230 [1967].

[2] M. T. FANG, D. A. FRASER, and J. E. ALLEN, Brit. J. Appl. Phys. **2**, 229 [1969].

[3] P. L. AUER, J. Appl. Phys. **31**, 2096 [1960].

[4] R. G. MCINTYRE, J. Appl. Phys. **33**, 2485 [1962]; Advanced Energy Conversion **2**, 405 [1962]; Proc. IEEE **51**, 760 [1963].

[5] N. I. IONOV, J. Techn. Fiz. **18**, 96 [1948].

The emision conditions of the diode are characterized by the quantitaties

$$\alpha = (\vec{N}_+/\vec{N}_-)_{\text{neg. emitter}},$$

the ratio of densities of the charge carriers leaving the negative plate and

$$\eta_d = e V_d/k T.$$

η_d denotes the diode voltage V_d in units of the thermal energy kT. Only the case $\eta_d > 0$ is considered. By interchanging the roles of both emitters, however, the case $\eta_d < 0$ is obviously described as well. If α is larger than unity the state of emission of the diode is said to be ion rich. The emission is electron rich if $\alpha < 1$. Generally, the quantity α was used to simplify the calculations of the hitherto existing theories. As a consequence, α is used here too, to facilitate comparison with the existing theories. It should be kept in mind, however, that α cannot be measured in practice.

It turns out to be convenient for the computations to introduce normalized variables $\eta = eV/kT$ and $\xi = x/L$ into Poisson's Eq. (1). The unit of length is chosen to be $L = (kT/8\pi e^2 \vec{N}_-(-\eta_d))^{1/2}$, a quantity defined analogous to the Debye-length

$$\lambda_D = (kT/8\pi e^2 N_p)^{1/2},$$

N_p being the plasma density. However, the quantity L varies in a complicated way with the working conditions of the diode. Therefore, all final results are given with the Debye-length as a unit length.

The distribution functions of the particles as well as the particle densities are sectionally monotonic explicit functions of $V(x)$ and $\eta(\xi)$ respectively. Therefore, instead of the distance coordinate ξ the normalized potential η can be used as the variable.

Consequently, the Poisson-Eq. (1) can be expressed in the normalized form

$$F'(\eta) = \vec{n}_-(\eta) + \beta \overleftarrow{n}_-(\eta) - \alpha \vec{n}_+(\eta) - \gamma \overleftarrow{n}_+(\eta), \quad (2)$$

with the definition

$$F(\eta) \equiv \eta'^2(\xi),$$

where the prime denotes differentiation with respect to the argument. The symbols denote:

$$\vec{n}_-(\eta) \equiv \vec{N}_-(\eta)/\vec{N}_-(-\eta_d),$$
$$\overleftarrow{n}_-(\eta) \equiv \overleftarrow{N}_-(\eta)/\overleftarrow{N}_-(+\eta_d),$$
$$\vec{n}_+(\eta) \equiv \vec{N}_+(\eta)/\vec{N}_+(-\eta_d),$$
$$\overleftarrow{n}_+(\eta) \equiv \overleftarrow{N}_+(\eta)/\overleftarrow{N}_+(+\eta_d),$$

$$\beta \equiv \overleftarrow{N}_-(+\eta_d)/\vec{N}_-(-\eta_d),$$
$$\gamma \equiv \overleftarrow{N}_+(+\eta_d)/\vec{N}_-(-\eta_d).$$

The two end plates ($T_I = T_{II}$) are assumed to emit identical Richardson current densities $\vec{j}_-(-\eta_d)$ and $\overleftarrow{j}_-(+\eta_d)$; consequently, $\beta \equiv \overleftarrow{j}_-/\vec{j}_- = 1$. On the other hand, for the ion current densities the expression

$$\gamma = \alpha \exp\{-\eta_d\}$$

holds [6].

Analytically, Eq. (2) can be integrated only once, yielding the electric field distribution in the diode. To obtain the potential distribution, this time a numerical integration has to take place. The formal solution is given by

$$\xi(\eta) = \int_{-\eta_d}^{\eta} (F(\eta))^{-1/2} \, d\eta. \quad (3)$$

At first, the ranges of existence of the various types of potential shapes in the parameter space (α, η_d) are defined and the numerical values of the characterizing quantities

- plasma potential η_p
- potential extremum η_e
- electric field intensity $(F(\pm\eta_d))^{1/2}$

in the vicinity of each of the emitters are computed. In a second step Eq. (3) is solved numerically for the ranges and data evaluated in this way; therefrom one obtains the actual potential distributions.

2. Theory

For the computations we have to distinguish between different types of potential distributions: uniform potential distributions within the plasma (Fig. 2) and spatially oscillatory potentials (Fig. 3). Po-

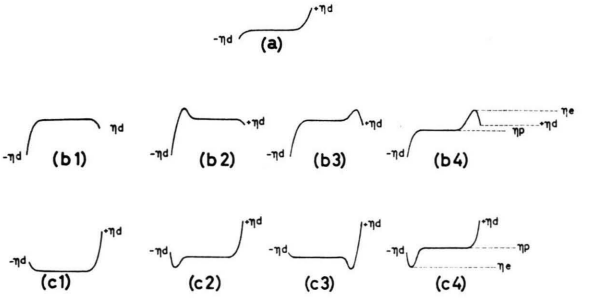

Fig. 2. Trial distributions of potential between the electrodes a) potential shape of type A, b) potential shape of type B, c) potential shape of type C.

[6] M. TROPPMANN, Report IPP 2/82, August 1969.

tential shapes of the first kind may be subdivided into monotonic and nonmonotonic distributions, either ion rich or electron rich near the emitters.

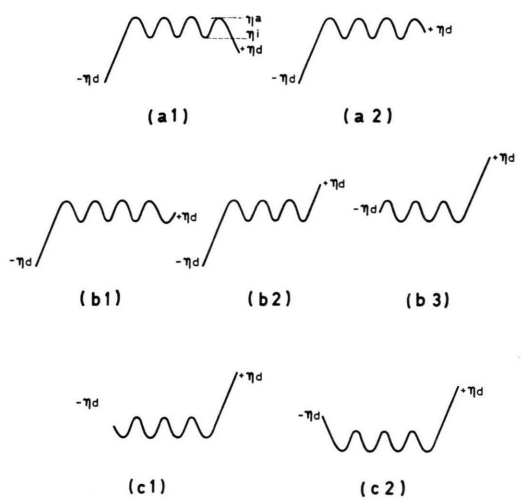

Fig. 3. Trial distributions of the spatially oscillatory potentials.

2.1. Potential Distributions with Uniform Plasma Potential

In order to enable the theoretical treatment of the model potential distributions we have to make an assumption concerning the extension of the emitter sheath. Physically the sheath boundary may be defined as the point where the potential gradient becomes smaller than statistical electric fields arising from thermal fluctuations. For the sake of simplicity thermal noise is neglected here; therefore, we define the sheath boundary by the equations

$$F'(\eta;\eta_d,\eta_e,\alpha)\big|_{\eta=\eta_p}=0 \tag{4}$$

and

$$F(\eta;\eta_d,\eta_e,\alpha)\big|_{\eta=\eta_p}=0\,, \tag{5}$$

i. e. we assume the body of plasma to be ideally free of space charge F' and electric fields F. The values of the characterizing quantities η_p, η_e and $F(\pm\eta_d)$ have to be determined in such a way that the integral in Eq. (3) results in the given value of the distance of the electrodes. Since the idealized conditions Eqs. (4) and (5) cannot be satisfied for finite distance this model can only be used with the assumption of infinite distance between the emitters. The influence of the opposite emitter on the sheath under consideration is provided by conditions on the current flowing in the plasma. If electric fields due to ohmic effects are neglected, the assumption of infinite diode spacing has no influence on the physical properties of the emitter sheath under consideration.

To obtain a first orientation we now compute the curves in parameter space dividing different regions where the types of potential shapes displayed in Fig. 2 are present.

Starting from the monotonic potential shape of type A (Fig. 2 a) we obtain the transition curves (Fig. 4 a) to the nonmonotonic distributions B and C respectively, from the condition that the derivative of the potential curve becomes zero at one of the emitter (see Fig. 4 b). If α is varied at constant diode voltage, transition A $\rightarrow$ B is characterized by vanishing electric field intensity $F=0$ and vanishing space charge density $F'=0$ at emitter E_{II}, whereas A $\rightarrow$ C is given by $F=0$, $F'\neq 0$ at E_I. The behaviour of both emitter sheaths differs for the following reason: both plates are emitting equal electron currents, whereas, since the potential distribution directs most of the ion flux from the plasma to the negative electrode, the ion production at the negative emitter exceeds that of the positive one. Furthermore, in the vicinity of plate I the ions always stay for a longer time than at E_{II}. It can be shown quantitatively that only near emitter I the space charge density can be forced to form a double sheath. In front of E_{II}, however, the emitter sheath changes from a simple electron sheath to a simple ion sheath while the potential distribution changes from type A to type B.

It is noticeable that these transition curves (Fig. 4) as well as the value of the plasma potential in case A can be computed numerically from one equation only. In the case of the nonmonotonic potential distributions (Fig. 2 b, c) however, the coupled Eqs. (4) and (5) have to be solved for the unknown quantities η_p and η_e. Using the usual methods of iteration, difficulties arise as a consequence of the limited ranges of definition of the functions involved. Therefore, we calculated the contour lines of the two four-parametric functions $F'(\eta_p,\eta_d,\eta_e,\alpha)$ and $F(\eta_p,\eta_d,\eta_e,\alpha)$ and looked for common zeros. By aid of this lengthy procedure *all* zeros must be found.

To achieve an impression of the variety of these zeros, Fig. 5 shows a three-dimensional representation of the cut surface of the function $F'=0$ and $F=0$. The values of η_p, η_e corresponding to potential distributions with monotonic and nonmonotonic emitter sheaths in the case of electron rich emission

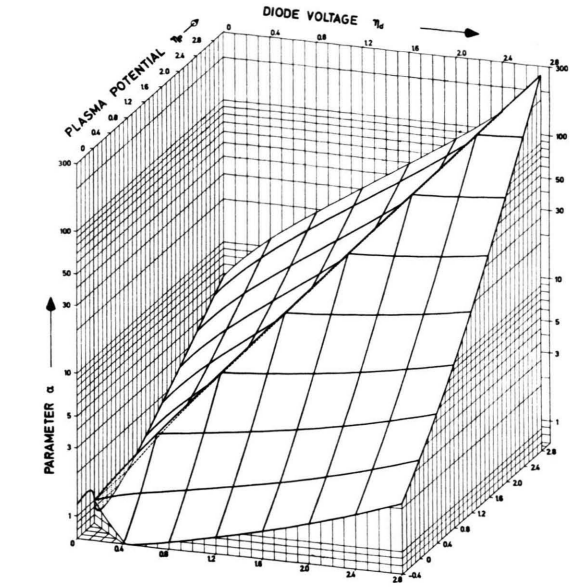

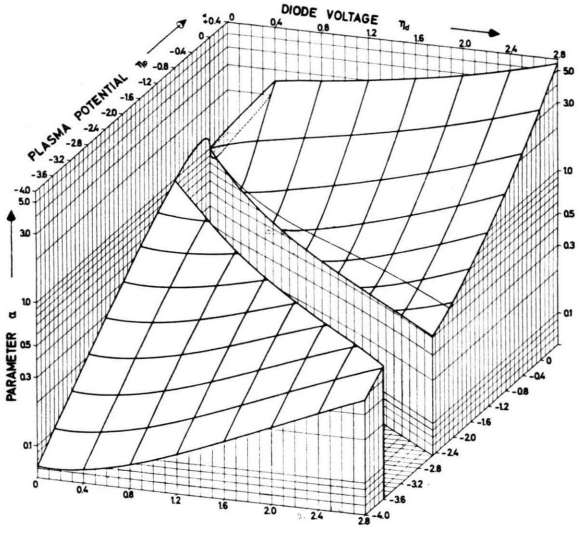

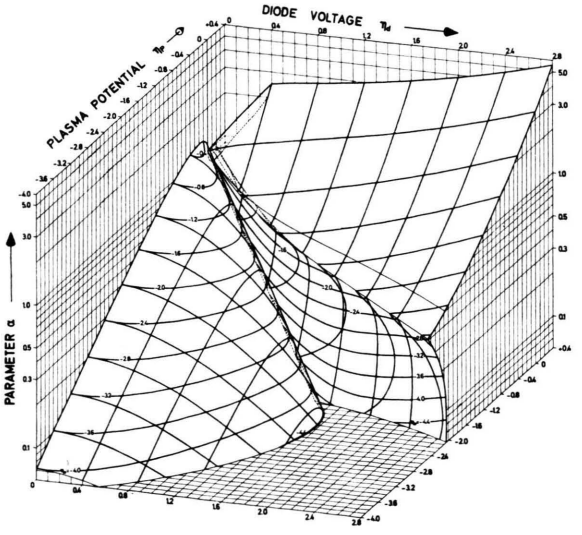

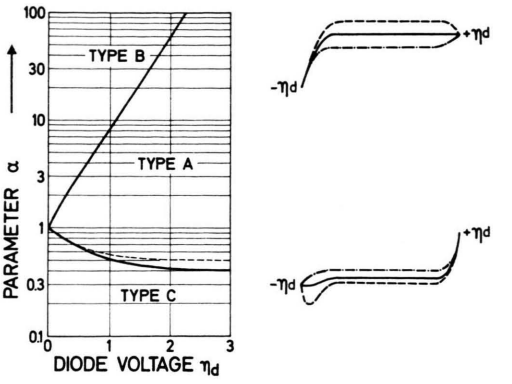

a) b)

Fig. 4. a) Regions of various potential distributions in parameter space. The broken line separates electron and ion sheaths in front of the negative emitter. b) Potential shapes at the transition from type A to types B and C respectively.

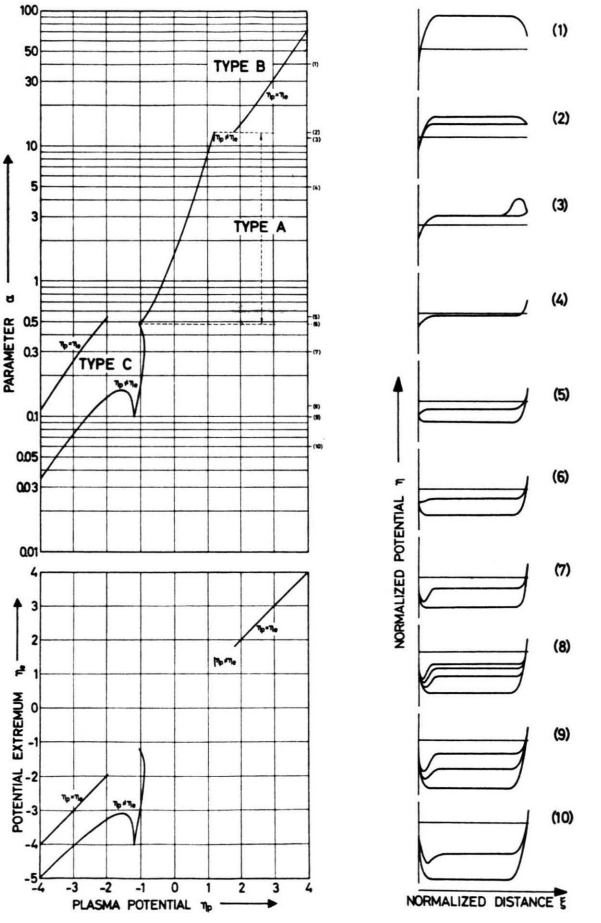

a) b)

Fig. 6. a) Cross-section of the solution surface (Fig. 5) parallel to the axis of the parameter α; $\eta_d = 1.2$; b) Potential distributions for various values of α (schematically).

← Fig. 5. Cut surface of the two equations $F' = 0$ and $F = 0$ (equations of the space charge density and of the electric field intensity at the plasma boundary). a) Ion rich emission, $\alpha > 1$; b) electron rich emission, $\alpha < 1$, $\eta_p = \eta_e$; c) electron rich emission, $\alpha < 1$, $\eta_p \neq \eta_e$.

are plotted separately, showing impressively the complexity of the cut surface. For the discussion of the physical significance of these common zeros of $F=0$ and $F'=0$ a cross-section parallel to the axis of parameter α is shown in Fig. 6 a. Fig. 6 b displays the various potential distributions (shown schematically) occurring if α is varied. The principal character of these results does not depend on the value of η_d; we choose $\eta_d = 1.2$. If $\alpha < 0.5$, there are always two potential shapes of type C: one with monotonic sheaths and the other one with a double sheath in front of the negative emitter, the plasma potential of which may be larger or smaller than the potential of the negative emitter.

One should keep in mind that these results are mathematical solutions, which do not take into account that the physical solutions have to fulfil the condition

$$F(\eta) \geqq 0 \tag{6}$$

i. e. that the square of the electric field intensity cannot be negative. Employing this condition we get a unique relation between η_p and α ($\eta_d = \text{const}$), with the exception of two discontinuities of η_p. Later on we shall discuss this point in more detail. In Fig. 7 the solutions compatible with (6) are shown with a solid line, whereas common zeros which do not satisfy condition (6) are represented by broken lines.

In the series of plots of Fig. 7 b actual potential distributions corresponding to the curves of Fig. 7 a are shown.

It should be emphasized that the well-known ambiguity of solutions in certain regions of the parameter space is reduced to a single solution by (6). To our knowledge, up to now this condition has been taken into acount only by FANG et al. [2, *].

2.2. *Spatially Oscillatory Potentials*

Whereas in the computation of the distributions with uniform plasma potential infinite distance between the electrodes had to be assumed, the "waves" of the spatially oscillatory potentials (Fig. 3) have to fit into a finite spacing. In this case the condition of vanishing space charge density [Eq. (4)] cannot be fulfilled; a quasi-neutral plasma in the usual sense does no longer exist in the diode. Therefore, the assumption of infinite spacing is no longer necessary. Hence, we have to calculate the values of (η_a, η_i, K) referring to the given set (α, η_d, ξ_d). If e. g. the potential shape of Fig. 3(a1) is considered, the number $2K$ of the "waves" is defined by

$$K = \frac{2\,\xi_d - \int_{-\eta_d}^{+\eta_d} W\,d\eta - \int_{+\eta_d}^{\eta_a} W\,d\eta + \int_{\eta_a}^{+\eta_d} W\,d\eta}{\int_{\eta_i}^{\eta_a} W\,d\eta} \tag{7}$$

where $W = (F(\eta))^{-1/2}$. The quantities η_a as well as η_i are unknown; in this case they are subject to the condition

$$\eta_a > \eta_i \geqq +\eta_d .$$

Should η_a equal η_i this shape is reduced to the distribution of type B [Fig. 2(b1)] with constant plasma potential. If the "amplitude" $(\eta_a - \eta_i)$ decreases the denominator of Eq. (7) obviously tends towards zero and consequently the value of K towards infinity.

Defining the ranges of existence of the various models of Fig. 3, it is easily shown analytically that

- the number of the models may be reduced to three [Figs. 3(a1), (b2), (c2)].
- the spatially oscillatory potentials are found within the whole parameter space (α, η_d) (Fig. 8).

The transition curves between either two shapes are determined in such a way that one of the extremal values equals one of the emitter potentials. By an expansion in series, the boundary is found to coincide with the transition curve between the types A and B of the distributions with uniform plasma potential (Fig. 4 a) if ion rich emission ($\alpha > 1$) is assumed. If $\alpha < 1$ it results that the range of existence of a distribution with electron sheaths near both emitters [Fig. 3(c2)] extends beyond the range of existence of type C up to the curve which separates ion and electron sheaths in front of the negative emitter (see broken line in Fig. 4 a). The transition curve between the shapes A and C is shown for comparison as a dashed line in Fig. 8.

It is emphasized explicitly that in this way only the ranges of existence are separated in which spatially oscillatory potentials are *possible*. Within the framework of the present theory it cannot be decided whether they really exist. This question could be answered only by a complicated investigation of stability involving the solution of the time-dependent Vlasov equation *and* the Poisson equation simultaneously.

* We became aware of this paper just after the computation of the actual potential distributions of type C had been completed.

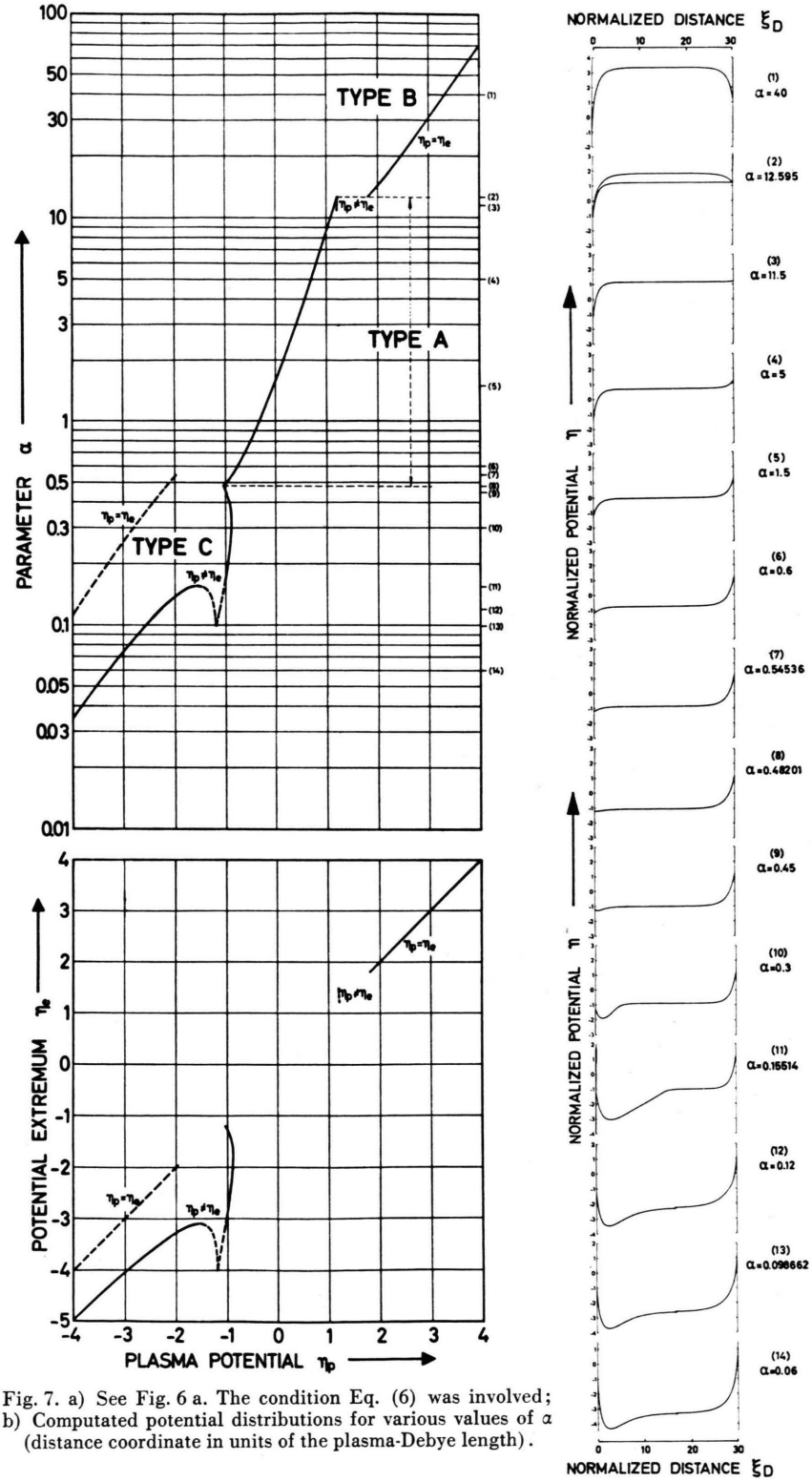

Fig. 7. a) See Fig. 6 a. The condition Eq. (6) was involved; b) Computated potential distributions for various values of α (distance coordinate in units of the plasma-Debye length).

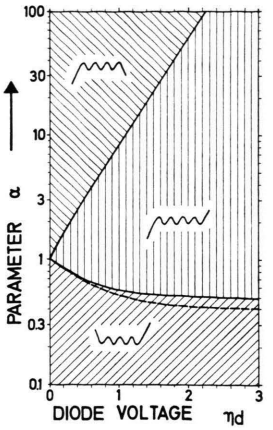

Fig. 8. Ranges of existence of the spatially oscillatory potentials.

3. Experimental Set-Up

Measurements were performed in the Cs-diode ELSA. Technical details of the machine are described in [7].

At the end plates (polycrystalline tantalum, spacing usually 2 – 3 mm) plasma was produced by contact ionization of a neutral cesium beam. The neutral particle density could not be controlled accurately because of insufficient wall cooling. So the diode was working usually in the vapor pressure mode, the neutral pressure being a function of the plate temperature.

We made use of an improved electron beam probing technique (Fig. 9) to measure the distribution of the electric field intensity in the plasma diode. To avoid the disadvantages of slit diaphragms formerly employed [8] a pencil shape electron beam passes parallel to the surfaces of the emitters through the gap in between. The beam is swept parallel to itself in a direction perpendicular to the emitter surface over the diode spacing by an electrostatic saw tooth deflection (Fig. 9), the frequency of which (≈ 2 kc/s) is high enough to resolve rapid changes in the diode potential distribution. This deflection is cancelled by an identical deflection system below the diode space. In this way, the resulting *narrow* beam comprises the information recorded at different points in a temporal sequence. The great advantage of this arangement as compared to all other probing techniques is that we can employ electron optical lens systems to magnify the small beam deflections caused by the diode field (e. g. as one of the simplest lens systems an electric quadrupole system may be used, the electric field intensity of which increases near the axis proportional to the radial distance). Finally the deflection within an electric cross-field (condensor 5 in Fig. 9), varying simultaneously with the deflection of the condensor system above the diode, again converts the temporal succession into spatial succession, thus projecting the distribution of the electric field intensity within the diode plasma in cartesian coordinates onto a fluorescent screen.

Another advantage of this probing technique is the following. The electron beam probe cannot be used if

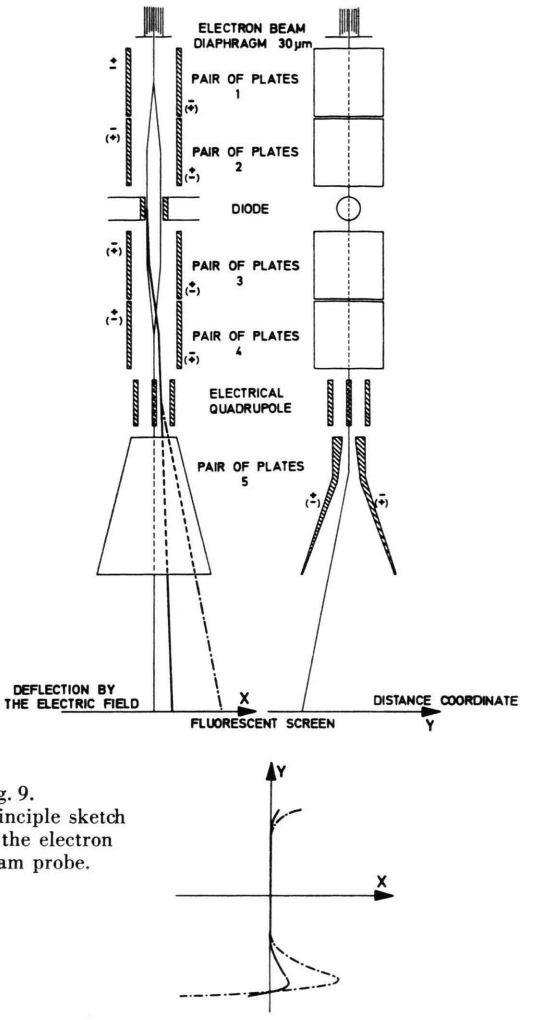

Fig. 9. Principle sketch of the electron beam probe.

electric field intensities should be investigated in the presence of strong magnetic fields. It is well-known, however, that in a given transversal electric field electrons as well as ions of *equal energy* are deflected by the same amount, whereas the ion deflection in a magnetic field is smaller by a factor of $(m_+/m_-)^{1/2}$ as compared to the electrons. The present technique using electrostatic deflection may therefore be used for an ion probe as well which allows probing of electric fields in the presence of magnetic fields.

To compare with theory either the experimental field curves have to be integrated or the theoretical potential profiles to be differentiated. We chose the second procedure because the differentiation of the theoretical curves is more exact and much easier to perform.

In order to classify the measured distributions of the electric field intensity the values of the quantities α as well as η_d must be known.

[7] M. TROPPMANN, Report IPP 2/79, July 1969.

[8] W. OTT, Report IPP 2/48, June 1966; Z. Naturforsch. **22 a**, 1057 [1967].

If the diode voltage V_d is normalized to the kinetic energy kT, η_d is easy to evaluate. Assuming ion and electron temperature to be equal to emitter temperature T_E, we have to measure V_d and T_E.

The actual voltage over the diode might be falsified by contact potentials. Both emitters consisting of the same material are operated at very high temperatures ($T_E \approx 2500\ ^\circ K$). Hence adsorption sheaths at the surfaces may be neglected. Consequently, the only error may arise from the variation of the work function across the surface of the emitters. After sufficient annealing this variation amounts to a few millivolts only [9] and may be neglected as well.

It is more difficult to measure the temperature of the end plates which, at a given heating power strongly depends on the distance between the emitters, being clearly most sensitive, if they are close together. To avoid these difficulties and to achieve a measurement independent of questionable values of $\varepsilon(\lambda)$ at small angles, black body radiation from a hole drilled in radial direction in the edge of the end plate was used to determine T_E. Two uncertainties, however, arise if such a procedure is used. The first one is that the relation between the temperature at the plate surface and at the bottom of the hole is not known accurately. Simultaneous measurements, with the second emitter removed, yielded differences not larger than 1 to 2 percent, based on common values of the emissivity for perpendicular incidence. Secondly, the hole disturbs the temperature distribution at the surface; the error may be of the same magnitude. Small azimuthal asymmetries in the temperature gradient do not cause drastic effects in the behaviour of the plasma when we are working without a magnetic field. Furthermore, the electron beam does not pass through parts in which temperature differences may occur.

Up to now no measurement of

$$\alpha \equiv (\vec{N}_+/\vec{N}_-)_{\text{neg. emitter}}$$

is known which is not subject to substantial doubt. α can only be estimated with large error. In the experiment the numerical value of α depends on the emitter temperature as well as on the neutral particle density. If the temperature of the end plates is being risen, α does not change proportionally to the RICHARDSON current; as in most of the Q-machines operating with cesium the neutral particle pressure rises too, because of insufficient cooling of the walls. By changing the emitter temperature rapidly, this undesired effect could be minimized, thus taking advantage of the thermal inertia of the container walls. We can, however, be sure that α is a *monotonically* decreasing function of the emitter temperature.

Varying the emitter temperature rapidly at a fixed value of the diode voltage, the sequence of distributions

[9] N. XUAN PHUC, B. HUTZLER, and T. ALLEAU, Int. Conf. on Thermionic Electrical Power Generation, London 1965, Section 6.

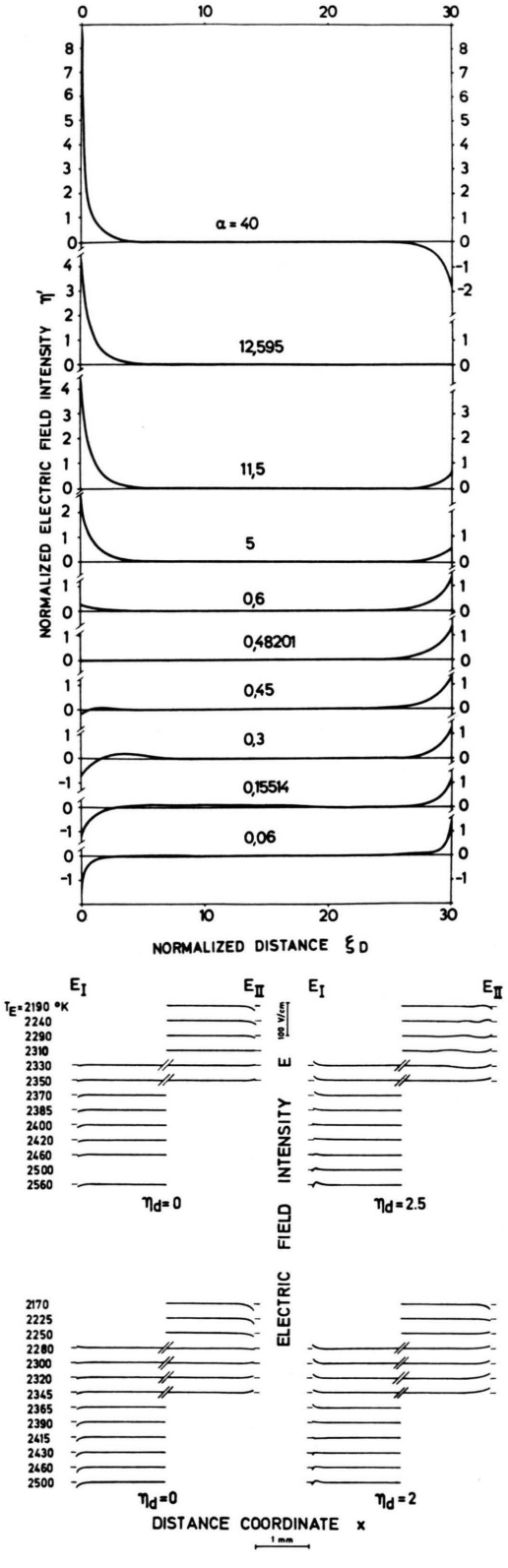

Fig. 10. Electric field curves for various values of α; η_d = const. a) Theory: $\eta_d = 1.2$; b) experiment: $\eta_d = 0$; $\eta_d = 2.5$ and $\eta_d = 2.0$ respectively.

of the electric field intensity obtained experimentally could be compared with the succession of various types of profiles given by the theory. The point $\alpha = 1$ is defined by the observable sudden change from a negative to a positive space charge sheath in front of the negative emitter.

4. Experimental Results

Theoretical and experimental results are compared under the following conditions:

a) α remains constant and the value of η_d is varied, or

b) vice versa.

From our computations we know that for electron rich emission ($\alpha < 1$) the sheath in front of the negative emitter changes its character if η_d is varied, whereas the sheath near emitter II only changes its potential drop. The situation is inverse if $\alpha > 1$. For that reason only those sheaths which change their character are investigated in detail.

For various values of α ($\eta_d = 1.2$) the theoretical curves of the electric field intensity are represented in Fig. 10 a. They correspond to the potential distributions shown in Fig. 7 b. In Fig. 10 b for comparison, a sequence of experimental profiles is given, measured while the emitter temperature had been varied from 2170 to 2560 °K at a constant diode voltage. In theory as well as in the experiment the curves of the sequence change their character in a similar manner. In front of the second emitter spatially oscillatory potential shapes are observed, the amplitude of the potential variation being damped with increasing distance from the ionizing surface. This behaviour will be discussed later on. If the diode voltage is varied at a fixed value of α (Figs. 12 and 13) oscillatory distributions appear more pronouncedly. Temporal diode oscillations occur which have the effect of smoothing the field curves if η_d approaches a value, causing electron saturation current to flow. NORRIS [10] and BURGER [11] could verify the onset of these diode oscillations by computer simulation: the potential distribution is not stationary but passes in rapid succession through various temporary dc-states.

If the emitter temperature is high enough, starting from a single electron sheath at $\eta_d = 0$ a space charge double sheath forms with increasing diode voltage (Fig. 11) corresponding to a change of the sign in the electric field intensity within the sheath region. According to the theory where only distributions of type C are posible if $\alpha < 0.5$ no transition to the monotonic potential distributions could be seen.

When the emitter temperature is reduced by about 270 °K we obtain the results of Fig. 12. The electron sheath near emitter E_I turns into an ion sheath with increasing voltage if η_d is varied again at $\alpha = \text{const}$. The ion sheath is being enlarged in front of the positive emitter. If η_d becomes larger than a critical value spatially oscillatory potential shapes appear. A wave crest moves from the diode plasma towards the emitter surface. Increasing voltage reduces the wave length, additional wave crests appear in the distributions. – With respect to the damping we refer to Section 5.

Similar results are found (Fig. 13) if ion rich emission is considered. Oscillating potentials appear as well. Their range of existence depends on the operating conditions of the diode. E. g. they accompany the change of the sign of the space charge sheath at the positive emitter and they are always present in the case of the monotonic distribution A.

Summing up, we find in the experiment the various profiles of the electric field intensity predicted by the theory if all collisions are neglected. The transitions between the modes are obvious and occur in the predicted sequence. It is astonishing to find the spatially oscillatory potentials in front of the positive emitter within limited ranges of the parameters varied in the experiment, whereas in theory they are possible at all conditions. The criterion reducing their range of existence could not be clarified. From the experiment, however, we get a hint leading to the following hypothesis: the wavy potentials are always damped; their amplitudes decrease with increasing distance from the positive emitter. The ions "born" there are accelerated in the emitter sheath. However, if they collide with plasma particles and lose part of their directed energy, some of them can be trapped within the potential throughs, thus reducing the inhomogeneities of the space charge.

In the following section we try to understand on the basis of a qualitative picture the complicated process of trapping and its consequences.

[10] W. T. NORRIS, J. Appl. Phys. **35**, 3260 [1964].

[11] P. BURGER, J. Appl. Phys. **36**, 1938 [1965].

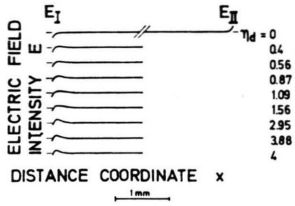

Fig. 11. Experimental electric field curves for $\alpha < 0.5$; $T_E = 2570\ ^\circ K$, $N_p = 8 \cdot 10^9\ cm^{-3}$.

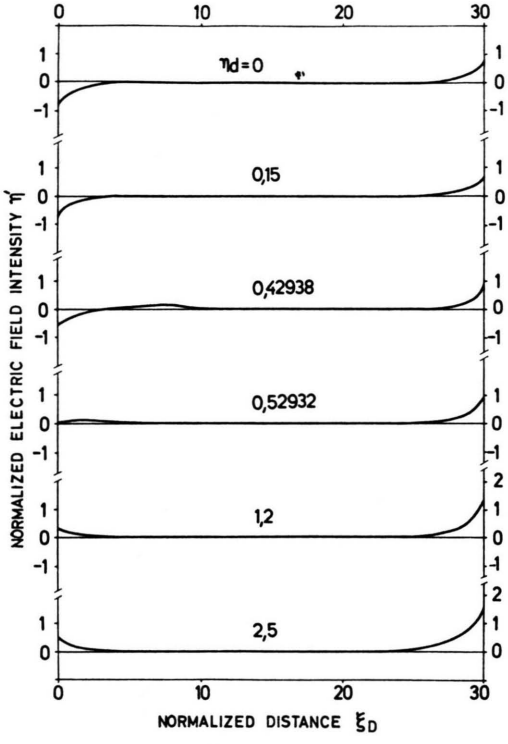

Fig. 12 a.

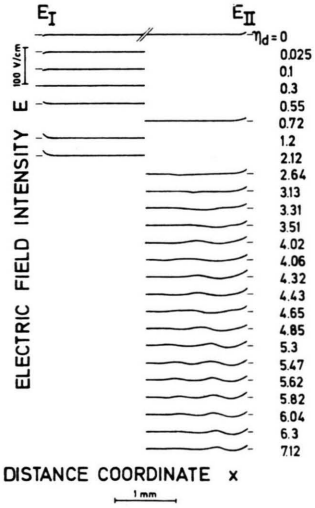

Fig. 12 b.

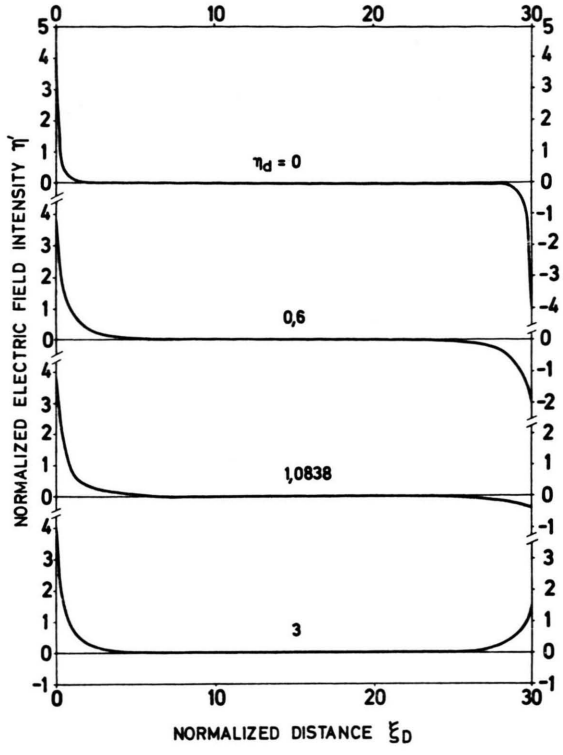

Fig. 13 a.

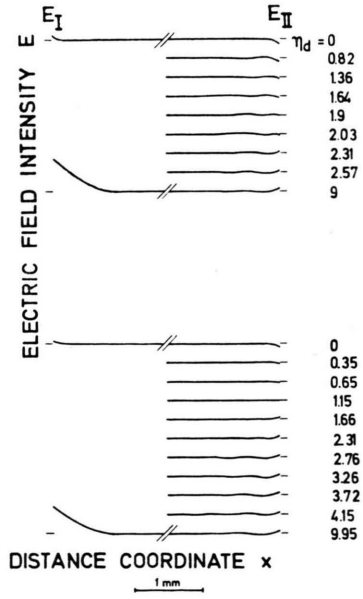

Fig. 13 b.

Fig. 13. See Fig. 12, $\alpha > 1$. a) Theory: $\alpha = 10$, b) experiment: above $T_E = 2270\ ^\circ K$, below $T_E = 2240\ ^\circ K$.

← Fig. 12. Electric field curves, $\alpha < 1$. a) Theory: $\alpha = 0.65$, b) experiment: $T_E = 2300\ ^\circ K$, $N_p = 4.8 \cdot 10^9\ cm^{-3}$.

5. Trapping of Particles

We mentioned above that by no means all common zerros of the space charge and the electric field Eqs. (4) and (5), respectively, could be accepted as physical solutions of Poisson's equation. Gaps appeared in the range of accessible values of η_p (Fig. 7). One of these discontinuities was found at electron rich emission, the other one at the transition from the monotonic distributions to the profiles of type B. What is the reason for these gaps? The potential distributions were calculated assuming the collisionless approximation which implies that the distribution functions of the particle velocities exhibit discontinuities and gaps. Neglecting collisions at all, means to neglect diffusion in velocity space and, hence, the capture of charged particles about a potential extremum. However, even if the collision time is much larger than the transit time of a particle through the diode the probability of collisions is finite. Therefore particles exist which travel in closed orbits in phase space never touching one of the emitter surfaces. These trapped particles may substantially change the space charge density and therefore the potential distribution.

Up to now no reasonable assumption of the velocity distribution function of the trapped particles does exist. KUCHEROV and RIKENGLAZ [21] set about the general problem of trapping, but could not handle the colision integral of the Boltzmann equation and had to be content with the special case of a Maxwellian velocity distribution of the trapped particles.

Studying the influence of these particles on the potential profiles with uniform plasma potential computated in Section 2, we assume that the particles are in thermal equilibrium with one of the emitters easily accessible to them. We also confine ourselves to the extremal case of filling up the gap in the velocity distribution functions entirely. In analogy to the foregoing procedure the potential distributions of Figs. 14 – 16 are calculated, based on these new assumptions. For comparison, we give the results of the collisionless theory in broken lines. The abrupt changes in the curve α vs. η_p disappear (Fig. 14 a). Filling up the gaps in the velocity distribution functions manifests itself in theory in reducing the absolute values of η_p, η_e as well as those of the electric field intensities. In the range of the profiles of type C the difference between the values of potential extremum and plasma potential, respectively, nearly disappears. In this way, we get a practically important result from these simple calculations: under real conditions, involving collisions, a nearly monotonic distribution of the potential within the sheath can be expected, a result which justifies the assumption of a monotonic potential drop in front of the emitters, usually employed in Q-machines.

Concerning the theory of the wavy potentials the spatial damping sugests an analogous effect. In fact, if thermalized velocity distributions are assumed, none of the oscillatory potentials can be found in the whole parameter space α vs. η_d. Thus we may conclude: spatially oscillatory potential shapes are characteristic for the collisionless diode. Their practical importance is limited, because it is hardly possible to realize the assumption of strictly collisionless conditions.

To test this model experimentally the collision probability of the charge carriers should be risen keeping other parameters constant. This can be done simply by introducing noble gas into the diode. For geometrical reasons it is obvious that the neutral atoms collide much more frequently with the hot emitter plates than with the plasma ions. The noble gas in the diode may therefore be assumed to be in thermal equilibrium with the plates. Thus by collision with noble gas atoms only the directed energy of the ions may be altered but *not* their temperature.

In Fig. 17 a set of measured electric field curves with slowly increasing neutral gas pressure is shown whereas other conditions are kept constant. An increasing of the wave length of the spatial oscillations can be seen immediately; at the same time their amplitudes decrease until finally no structure of the electric field can be detected **. If the noble gas is pumped out again the original distribution reinstalls.

In theory, if $\eta_p = \text{const}$, the introduction of thermalized velocity distribution functions does not only lead to suppressed oscillatory potentials, but also to a reduction of the electric field intensity within the sheath. To verify this second prediction a fur-

[12] R. YA. KUCHEROV and L. E. RIKENGLAZ, Sov. Phys.-Techn. Phys. **7**, 941 [1963].

** Sensitivity: the beam width on the screen was equivalent to a field intensity of 3 V/cm.

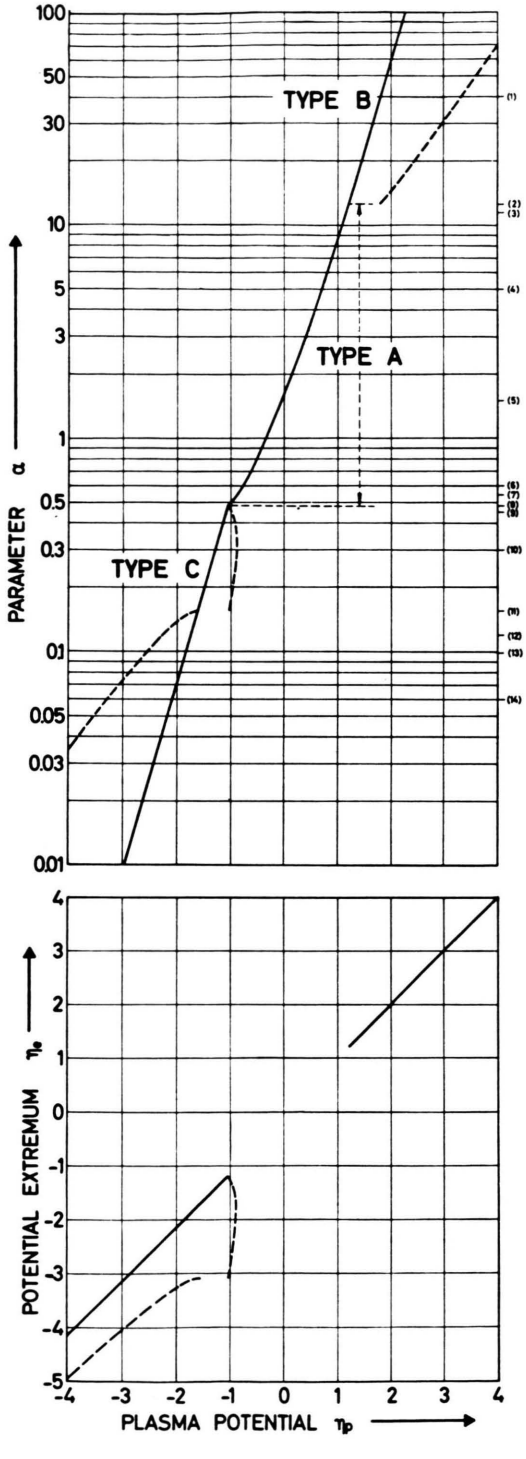

Fig. 14 a. ↑

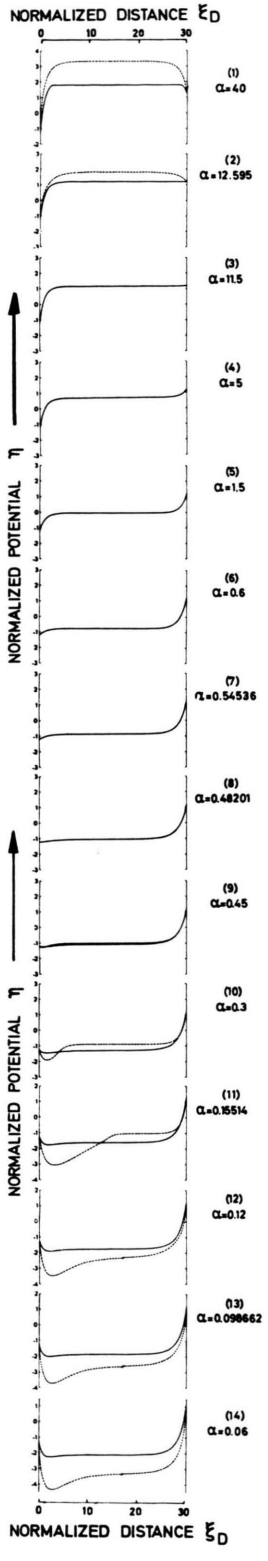

Fig. 14 b. →

Fig. 14. a) Solutions of the Eqs. (4) and (5). The trapping of ions near the potential extrema was involved; $\eta_d = 1.2$. b) Computated potential curves for various values of α (distance coordinate in units of the plasma Debye length). The broken lines indicate the solutions of the collisionless theory.

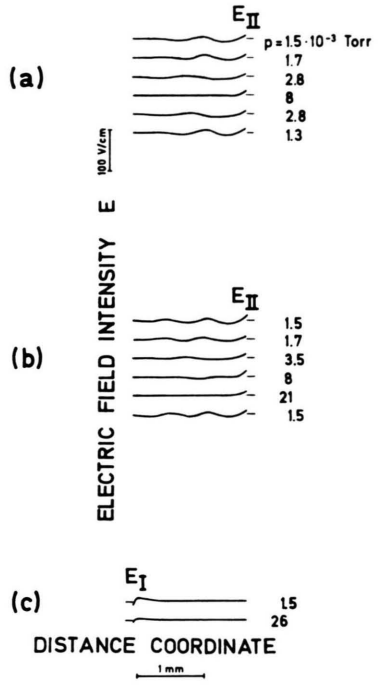

Fig. 17. Effect of the neutral pressure on the distribution of the electric field intensity.
a) Xe: $T_E = 2300\ ^\circ K$, $\eta_d = 4.16$,
b) Ar: $T_E = 2300\ ^\circ K$, $\eta_d = 4.28$,
c) Ar: $T_E = 2560\ ^\circ K$, $\eta_d = 1.15$.

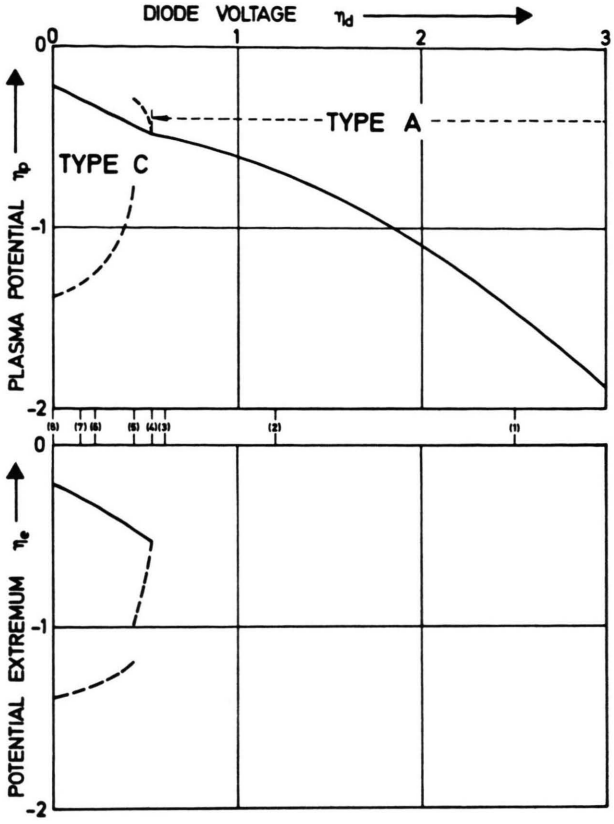

Fig. 15 a.

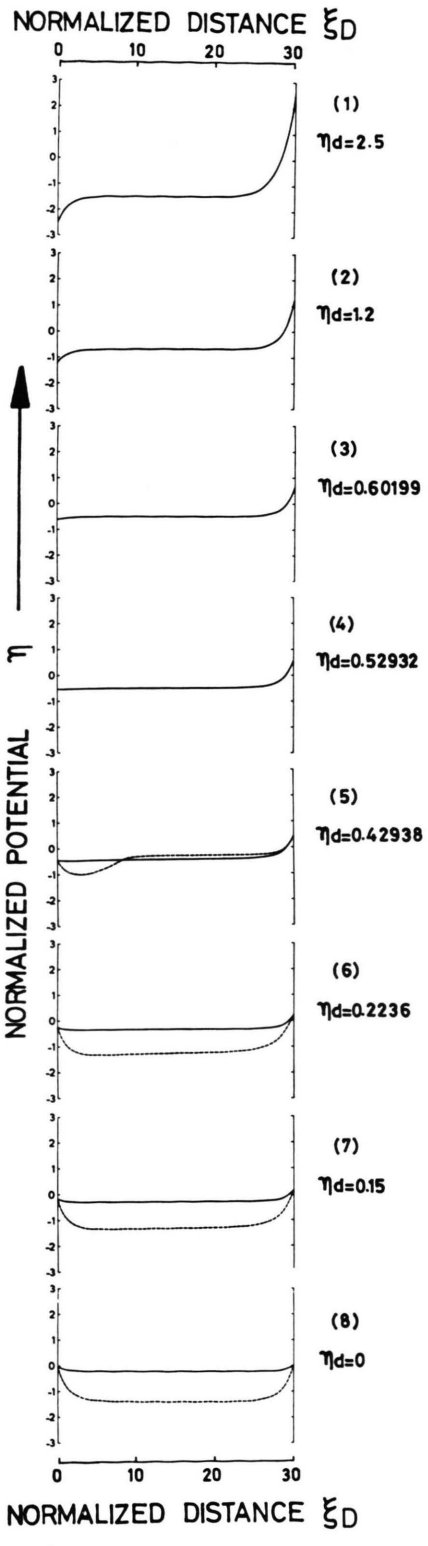

Fig. 15. a) See Fig. 14 a; $\alpha=0.65$; b) actual potential distributions for various values of η_d.

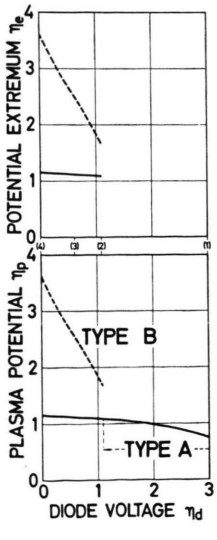

Fig. 16 a.

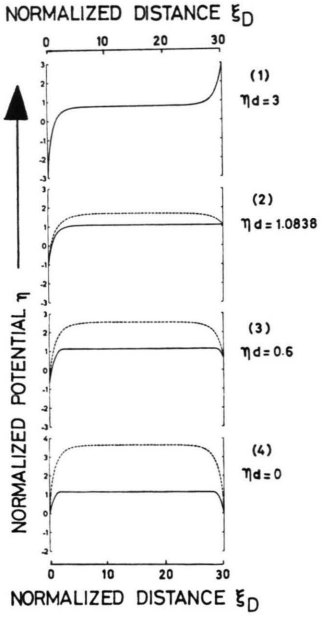

Fig. 16 b.

Fig. 16. See Fig. 15; $\alpha=10$.

ther experiment was performed in an analogous way; the diode, however, was operated under conditions where wavy potentials did not occur in the collisionless case. The results are presented in Fig. 17 c. According to theory the electric field intensity is reduced with increasing neutral pressure.

In a more quantitative approach we estimate the collision frequency necessary for suppressing the wavy potentials. From Fig. 17 we learn that they vanish at a pressure of 10^{-2} Torr which corresponds to a ion-neutral collision frequency

$$\nu_{in} = N_0 \pi p^2 \langle v \rangle \approx 2.8 \cdot 10^4 \text{ s}^{-1}$$

and to a mean free path

$$\lambda_{in} = \langle v \rangle / \nu_{in} \approx 2 \text{ cm},$$

where $\langle v \rangle = (8 k T / \pi m_+)^{1/2}$ and p denotes the impact parameter. Therefrom we may calculate

$$P \equiv \frac{\text{distance between the emitters}}{\text{mean free path } \lambda_{in}} \approx 0.1 .$$

Hence a collision probability of the order of 1/10 per transit seems to be sufficient for suppressing the wavy potentials. The critical value of $P \approx 0.1$ is expected to give the right order of magnitude for the special conditions of this experiment; it is, however, certainly not correct in the *whole* parameter range. Experimental evidence shows that the oscillatory potential shapes are more likely at a higher voltage, less probable at a lower one. Furthermore, as far as $\eta_d = 0$ is concerned even in the absence of a noble gas only distributions with uniform plasma potential were observed.

In this estimation we asumed that the damping of the oscillatory potential distributions is caused by collisions of plasm ions with particles of roughly the same mass. This assumption acquires a higher degree of plausibility by the following argument:

According to this assumption, the ion-ion collisions already present in the diode before introducing neutral gas should cause a certain "damping rate" for the oscillatory potentials. If this is true, first indications of further damping by ion-neutral collisions should become noticeable at a neutral gas pressure where both collision frequencies are equal.

In experiment, at a given ion density, the first smoothing of the electric field curves was observed at a pressure of $2 \ldots 3 \cdot 10^{-3}$ Torr, corresponding to

$$\nu_{in} \approx 6 \ldots 8 \cdot 10^3 \text{ s}^{-1}.$$

In fact, with the ion density prevailing in experiment, the ion-ion collision frequency according to SPITZER's formula [13] is

$$\nu_{ii} = \frac{N_+ Z^4 \ln \Lambda}{11.4 A^{1/2} T_+^{3/2}} \approx 6 \cdot 10^3 \text{ s}^{-1} .$$

Summarizing, even a few collisions between ions and neutral particles are sufficient to suppress spatially oscillatory potential shapes. If the collision frequency is not too low it results that the profile with $\eta_p = \text{const}$ is more likely to occur than the (theoretically possible) oscillatory potential distribution.

6. Conclusion

a) At a given set of parameters the theory of the collisionsless diode together with the physically evident condition $E^2 \geqq 0$ results in a single potential profile with uniform plasma potential. At the same time an infinite number of spatially oscillatory potentials may exist, if one neglects collisions at all. The question of a theoretical selection criterion between these two possibilities is not discussed in this paper.

b) Using a new electron beam probing technique the sequences of potential distributions, appearing if one of the characteristic parameters α and η_d respectively is varied, could be verified experimentally in agreement with theory. Within small ranges of operating parameters of the diode wavy potentials were found, the amplitudes of which appeared more and more damped with increasing distance from the positive emitter. We suggested charge carriers to be trapped near the potential extrema.

c) The solutions of Poisson's equation were again calculated in the second part of the paper assuming fully thermalized velocity distribution functions for the trapped particles. Within this simplified model the wavy potentials were no longer existent, whereas the profiles with uniform plasma potential retained their characteristic properties; the absolute values of the potentials, however, were reduced. In order to verify this model, noble gases (Ar, Xe) were introduced into the diode thereby enhancing the collision frequency of the ions only without changing the characteristic parameter α.

[13] L. SPITZER, JR., Physics of Fully Ionized Gases, 2nd Ed., Intersci. Publ., New York 1962.

d) Spatially oscillatory potential turned out to be a feature of the strictly collisionless model only. For real plasma diodes solutions with uniform plasma potential are more probable. By rising the collision frequency of the ions the potential minimum in the case of the nonmonotonic potential distributions was reduced so much that it could hardly be noticed. This result is relevant for the theory of the Q-machine. Under normal conditions the assumption of a monotonic potential shape within the emitter sheaths of Q-machines seems to be a fair approximation.

Acknowledgements

The author is indebted to Priv.-Doz. Dr. E.W. BLAUTH and Dr. G. VON GIERKE for their interest and support. Numerous discussions with Drs. E. GUILINO and W. OTT in the course of this work have been of considerable value in clarifying certain points. The author also wishes to thank Mr. P. PIOTROWSKI and Mrs. H. WILHELM for their help in programming the numerical calculations. The assistance of Mr. J. KONRAD in technical work and during the measurements is acknowledged.

This work was performed as part of the agreement between the Institut für Plasmaphysik GmbH, Munich-Garching, and Euratom to conduct joint research in the field of plasma physics.

Abschätzung der für die Ionenextraktion wichtigen Parameter der Raumladungsschicht

K. FETTE und J. HESSE

Institut A für Physik der Technischen Universität Braunschweig

(Z. Naturforsch. **25 a**, 518—524 [1970]; eingegangen am 27. September 1969)

Ions extracted from a plasma often have to pass a space charge existing in front of the container wall. If collisions occur within the sheath, both, the ion composition and the extraction efficiency may heavily be influenced.

The parameters of interest are the extension and the field strength of the sheath. A theory is presented by which these quantities can be calculated.

The theory holds for a positive space charge, the orifice being biased negativ with respect to the plasma potential.

Numerical results are given concerning a weekly ionized nitrogen plasma.

In einer früheren Arbeit [1] konnte experimentell gezeigt werden, daß der Prozeß der Ionenextraktion durch die Existenz einer Raumladungsschicht vor der Extraktionssonde modifiziert wird. Es wurden sowohl Auswirkungen der Schicht auf den Ablauf von Ion-Molekül-Reaktionen als auch auf die Richtungsverteilung der austretenden Ionen nachgewiesen.

Ebenso ist bekannt, daß als Folge der Existenz der Raumladungsschicht auch die Transparenz der Extraktionsöffnung beeinflußt wird [2, 3].

Um die genannten Einflüsse der Raumladungsschicht abschätzen zu können, ist es notwendig, konkrete Vorstellungen über die räumliche Ausdehnung und die elektrische Feldstärke der Schicht zu haben.

Es wurde daher eine einfache Sondentheorie entwickelt, die es gestattet, zu konkreten numerischen Aussagen zu gelangen. Die Theorie gilt für eine überwiegend positive Raumladungsschicht, in der die Ionenbewegung stoßbestimmt ist.

Wegen der sondentheoretischen Behandlung ist die Rechnung für den in der Praxis häufigen Fall anwendbar, in dem die Extraktionsöffnung in einer ebenen Langmuir-Sonde angebracht ist.

Die Raumladungsschicht als Plasmabegrenzung

Befindet sich ein quasineutrales Plasma [4] im Kontakt mit einer Wand, und sind Elektronen die dominierenden negativen Ladungsträger, so bildet sich vor der Wand eine positive Raumladung aus. Diese nach LANGMUIR [5] benannte Raumladungsschicht ist die Folge der unterschiedlichen thermischen Geschwindigkeiten der Elektronen und Ionen. Im allgemeinen überwiegt der thermische Wandstrom der

Sonderdruckanforderungen an Priv.-Doz. Dr. H. H. BRÖMER, Institut für Physik, Technische Hochschule Braunschweig, *D-3300 Braunschweig*, Mendelssohnstr. 1 A.

[1] H. H. BRÖMER u. J. HESSE, Z. Naturforsch. **23 a**, 1960 [1968].

[2] G. HINZPETER, Ann. Phys. (Lpz.) **17**, 343 [1966].

[3] H. H. BRÖMER u. K. FETTE, erscheint demnächst.

[4] M. A. UMAN, Introduction to Plasma Physics, McGraw-Hill, New York 1964.

[5] I. LANGMUIR u. H. M. MOTT-SMITH, Phys. Rev. **28**, 727 [1925].